Journal of Applied Physics

RESEARCH ARTICLE | APRIL 25 2023

Trapping proteins on nanopores by dielectrophoresis

Special Collection: Solid-Liquid Interfaces: Atomic-Scale Structure and Dynamics

Taylor Colburn ; Dmitry V. Matyushov

Check for updates

Journal of Applied Physics 133, 164701 (2023)
https://doi.org/10.1063/5.0144564

View Online
Export Citation
CrossMark

Downloaded from http://pubs.aip.org/aip/jap/article-pdf/doi/10.1063/5.0144564/17001652/164701_1_5.0144564.pdf


Time to get excited.
Lock-in Amplifiers – from DC to 8.5 GHz

Find out more
Zurich Instruments

AIP Publishing

Journal of Applied Physics ARTICLE scitation.org/journal/jap

Trapping proteins on nanopores by dielectrophoresis

Cite as: J. Appl. Phys. **133**, 164701 (2023); doi: 10.1063/5.0144564
Submitted: 30 January 2023 · Accepted: 7 April 2023 ·
Published Online: 25 April 2023

View Online Export Citation CrossMark

Taylor Colburn[1] and Dmitry V. Matyushov[2,a)]

AFFILIATIONS

[1]Department of Physics, Arizona State University, P.O. Box 871504, Tempe, Arizona 85287-1504, USA
[2]School of Molecular Sciences and Department of Physics, Arizona State University, P.O. Box 871504, Tempe, Arizona 85287-1504, USA

Note: This paper is part of the Special Topic on Solid-Liquid Interfaces: Atomic-Scale Structure and Dynamics.
a)Author to whom correspondence should be addressed: dmitrym@asu.edu

ABSTRACT

Interest in the phenomenon of dielectrophoresis has gained significant attention in recent years due to its potential for sorting, manipulation, and trapping of solutes, such as proteins, in aqueous solutions. For many decades, protein dielectrophoresis was considered impossible, as the predicted magnitude of the force arising from experimentally accessible field strengths could not out-compete thermal energy. This conclusion was drawn from the mainstay Clausius–Mossotti (CM) susceptibility applied to the dielectrophoretic force. However, dielectric interfacial polarization leading to the CM result does not account for a large protein dipole moment that is responsible for the dipolar mechanism of dielectrophoresis outcompeting the CM induction mechanism by three to four orders of magnitude in the case of proteins. Here, we propose an explicit geometry within which the dipolar susceptibility may be put to the test. The electric field and dielectrophoretic force are explicitly calculated, and the dependence of the trapping distance on the strength of the applied field is explored. A number of observable distinctions between the dipolar and induction mechanisms are identified.

Published under an exclusive license by AIP Publishing. https://doi.org/10.1063/5.0144564

I. INTRODUCTION

Dielectrophoresis (DEP) is a general phenomenon in which a neutral particle experiences a force from a nonuniform electric field,[1–4] in contrast to the electrophoretic force acting on a charged particle. The DEP force is not strictly speaking a mechanical force as it arises from the dependence of the free energy of the particle in a nonuniform external field on its position. The free energy in the field $\mathscr{F}_E(\mathbf{r})$, depending on the particle coordinate $\mathbf{r}$, is a special case of the potential of mean force. The spatial gradient of the particle's chemical potential specifies the thermodynamic force[5,6] $\mathbf{f}_{\rm DEP} = -\nabla\mathscr{F}_E$ involving an entropic component and depending on the thermodynamic state.[7,8] We show below that $\mathbf{f}_{\rm DEP} \propto T^{-1}$ when the particle permanent dipole dominates in the DEP response, in contrast to mechanical forces which are independent of temperature.

The origin of the polarization free energy is the interaction of the average dipole moment at the particle $\langle\mathbf{M}_0\rangle_E$ with the (Maxwell) electric field $\mathbf{E}$ in the dielectric medium

$$\mathscr{F}_E = -\frac{\varepsilon_s}{2}\langle\mathbf{M}_0\rangle_E \cdot \mathbf{E}, \tag{1}$$

where ε_s is the dielectric constant (relative electric permittivity[9]) of the medium.

The neutral particle is viewed as being polarizable, that is, the dipole moment $\langle\mathbf{M}_0\rangle_E = \langle\mathbf{M}_0\rangle$ is zero in the absence of the field and is proportional to the field in the lowest order in E,

$$\langle\mathbf{M}_0\rangle_E \propto \mathbf{E}. \tag{2}$$

Substituting Eq. (2) into Eq. (1) and taking the spatial derivative of the electrostatic free energy yields the DEP force proportional to

Downloaded from http://pubs.aip.org/aip/jap/article-pdf/doi/10.1063/5.0144564/17001652/164701_1_5.0144564.pdf

the gradient of the electric field squared,

$$\mathbf{f}_{\mathrm{DEP}} = \varepsilon_0 \chi_{\mathrm{DEP}} \nabla E^2, \tag{3}$$

where $\varepsilon_0 \simeq 8.854 \times 10^{-12}$ (F/m) is the vacuum permittivity. By the fact of relating the force to the external field squared, the DEP susceptibility χ_{DEP} is a nonlinear[10] (quadratic) transport coefficient. Calculation and measurement of χ_{DEP} is the main challenge to the theoretical understanding of DEP in application to separation of particles of the nanometer length scale.

It is convenient to scale the DEP susceptibility with the dimensionless polarization parameter K,

$$\chi_{\mathrm{DEP}} = \frac{3}{2} \varepsilon_s \Omega_0 K. \tag{4}$$

Here, $\Omega_0 = (4\pi/3)R_0^3$ is the volume of a particle represented by a sphere with the effective radius R_0. The standard procedure to evaluate $\langle \mathbf{M}_0 \rangle_E$ and χ_{DEP} involves solving the Maxwell boundary-value problem[9] for the polarization of the surface dividing the dielectrics assigned to the particle from the surrounding medium. This solution leads to the polarization factor $K = K_{\mathrm{CM}}$ specified by the Clausius–Mossotti (CM) form[4,11,12]

$$K_{\mathrm{CM}} = \frac{\varepsilon_p - \varepsilon_s}{\varepsilon_p + 2\varepsilon_s} \simeq -\frac{1}{2}. \tag{5}$$

It is constructed with the dielectric constants of the protein, ε_p, and the solvent, ε_s; the common condition $\varepsilon_p \ll \varepsilon_s$ leads to second approximate relation.

Given that $K = K_{\mathrm{CM}}$ in Eqs. (4) and (5) depends only on the dielectric constants at the dielectric interface, the DEP susceptibility scales linearly[13] with the volume of the particle or proportionally to the cube of particle's effective radius R_0,

$$\chi_{\mathrm{DEP}}^{\mathrm{CM}} = \frac{3}{2} \varepsilon_s \Omega_0 K_{\mathrm{CM}} \propto R_0^3. \tag{6}$$

The particle size is the most significant parameter in defining the DEP force in Eq. (6). When applied to proteins, their relatively small size, $R_0 \sim 1$ nm, yields a force too low to trap a protein at the practical field strength $E \leq 10$ V/μm.[14–17] Nevertheless, Washizu *et al.* demonstrated protein trapping with fields $E \sim 1$ V/μm (3 V/μm in Ref. 18), an order of magnitude smaller than expected.[19] This observation had remained puzzling[20] until it was recognized that a large intrinsic permanent dipole moment of a protein produces an induced dipole $\langle M_0 \rangle_E$ nearly four orders of magnitude higher than what follows for the induced dipole from the CM factor.[21] The DEP susceptibility from the permanent dipole moment was also predicted to carry a sign of the polarization factor K opposite to that from Eq. (5): positive from the protein dipole vs negative for the CM factor. This theoretical result justified previously reported trapping of protein by DEP[18,19,22] connecting to a number of potential systems where such effects can be realized.[11,17,23–28] It is now increasingly appreciated that DEP susceptibilities of proteins are mostly consistent between different reports[11,26,29] and do not follow dielectric predictions based on the CM factor.[29–32] The reported instances of negative protein DEP can be traced back to aggregation as the CM induction mechanism becomes dominant for sufficiently large aggregates (see below).

The electric field magnitude required for trapping the protein can be estimated by a balancing condition equating the magnitude of the free energy $|\mathscr{F}_E|$ to the thermal kinetic energy $(3/2)k_{\mathrm{B}}T$ of the particle.[11,19,33] The resulting equation for the trapping field strength is

$$E_{\mathrm{trap}} \simeq (\beta \varepsilon_0 \varepsilon_s \Omega_0 K)^{-1/2} \simeq \frac{38}{\sqrt{K R_0^3}}. \tag{7}$$

Here, the field is in V/μm and $K = |K_{\mathrm{CM}}|$ for the negative DEP in the CM model [Eq. (5)] or $K = K_d$ for positive DEP due to protein's dipole as discussed below. The second approximate relation is estimated for $\varepsilon_s \simeq 78$ of the aqueous solution and $T = 300$ K; R_0 is in nm. For the parameters of lysozyme in Table I with $K = K_d$, one obtains $E_{\mathrm{trap}} \simeq 0.3$ V/μm.

The purpose of the present article is to offer a simple trapping geometry that may allow testing theory predictions and potentially be applied to building practical trapping devices. The gradient of the electric field is produced by a circular solid-state nanopore[34–36] cut through a conducting plate of a plane capacitor with the asymptotic electric (Maxwell) field E_{app} in its lower part (Fig. 1). Applying this condition to a particle carrying the permanent dipole M_0 and positioned at the symmetry axis of the nanotrap in Fig. 1, one obtains the following condition for the trapping distance z^* along the z axis (see below for details):

$$\frac{z^*}{d} = \left(\frac{4\beta \Omega_0 \varepsilon_0 \varepsilon_s K}{9\pi^2} \right)^{1/6} E_{\mathrm{app}}^{1/3}. \tag{8}$$

Substituting fundamental constants, one obtains

$$\frac{z^*}{d} = 0.22 \times \left(\frac{\varepsilon_s K}{T} \right)^{1/6} R_0^{1/2} E_{\mathrm{app}}^{1/3}, \tag{9}$$

where E_{app} is in V/μm, temperature T is in K, and the radius R_0 is in nm. The analytical result in Eq. (8) is obtained in the dipolar limit of the full analytical solution discussed below. Figure 2 compares Eq. (8) to the full solution showing that the dipolar approximation is accurate at $z^*/d > 1$.

The trapping distance z^* reaches zero value, that is, the protein is trapped at the center of the aperture, at the applied field

$$E_{\mathrm{app}}^* = 6.7 \times 10^2 \frac{1}{\sqrt{\varepsilon_s K R_0^3}}, \tag{10}$$

where the field is in V/μm and R_0 is in nm. This threshold electric field can be viewed as the lowest field in the capacitor device to allow protein trapping. This value becomes equal to $E_{\mathrm{app}}^* \simeq 0.5$ V/μm with the parameters of lysozyme in Table I.

Our discussion starts with a review of the standard polarization model of DEP [Eq. (5)] and the model based on induced orientation of the molecular permanent dipole.[21] These results are applied to deriving trapping conditions on a circular nanopore

Downloaded from http://pubs.aip.org/aip/jap/article-pdf/doi/10.1063/5.0144564/17001652/164701_1_5.0144564.pdf

Published under an exclusive license by AIP Publishing

TABLE I. Dielectric and DEP data for proteins in solutions.

Protein	M_p[a] (kDa)	$\Delta\varepsilon_{sol}/c_0$[b] ($mM^{-1}$)	K_d[c]	χ_c[d]	M_0, D	R_0 (nm)[e]	y_0
Ubiquitin (Ubiq)	8.6	3.82	8 354	1.08	221	1.37	153
Cytochrome *c* (Cyt-c)	13	6.70	6 643	1.09	238	1.87	70
Lysozyme (Lys)	14.3	1.75	3 751	1.20	208	1.79	61
Trypsin (Tryp)	23	6.74	7 126	1.30	271	2.0	74
Carboxypeptidase (Carb)	34	37.24	28 464		569	2.12	275
Hemoglobin (Hb)	64	26.9	12 155	1.12	495	2.57	115
BSA[f,g]	66	1.11	3 849	1.13	384	3.31	33
Concanavaline (Conc)	102	15.31	16 474		433	1.91	217
IgG[f]	150	25.9	4 552	1.14	840	4.3	70

[a]Molecular mass.
[b]Taken from Refs. 11 and 12 and other experimental data as explained in the supplementary material.
[c]From experimental data [Eq. (29)]; $\varepsilon_s = 78.4$ and $\varepsilon_\infty = 3.2$.
[d]Estimates from dielectric measurements [Eq. (31)].
[e]Protein radii are calculated in the supplementary material.
[f]BSA = bovine serum albumin, IgG = immunoglobulin G.
[g]Recent measurements[28] involving a eDEP trapping configuration report $K = 402$ (Lys) and 5 (BSA). The calculated ∇E^2 and E_{trap} were not corrected for electrolyte screening. If the energy balance condition in Eq. (7) with reported E_{trap} is applied, one obtains $K = 32$ (Lys) and 1.4 (BSA).

(Fig. 1). The dipolar DEP susceptibility χ_{DEP} has not been directly measured so far, but an alternative route based on solution dielectric measurements has been identified.[31,32] We conclude with outlining predictable consequences of the model and critical experiments that can be used to distinguish between dielectric polarization and dipolar orientational mechanisms of DEP. The present model does not account for the polarization of the double electrolyte layer around the protein[37] and, therefore, is limited, in practical applications, by frequencies of the applied field exceeding ~1 kHz.[29]

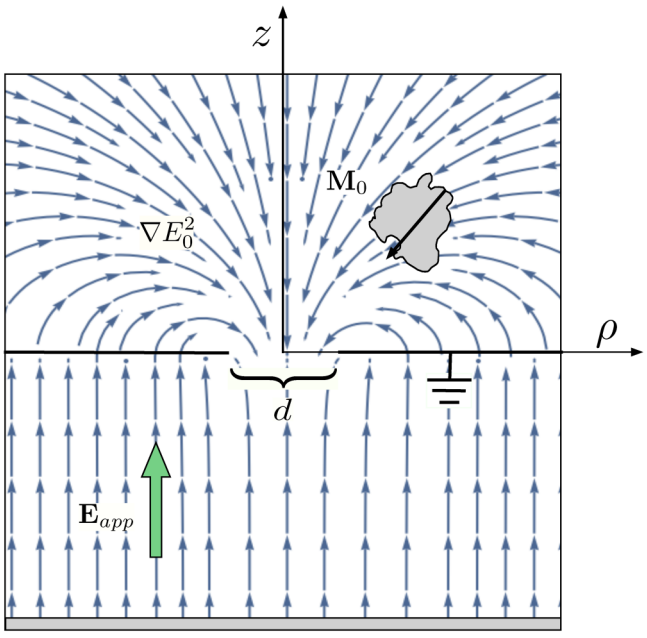

FIG. 1. Diagram of the nanotrap. A uniform field is applied to a grounded conducting plane with a circular hole. A dilute solution flows through the top chamber with the velocity **v**. Near the aperture, the protein molecule carrying the permanent dipole $\mathbf{M}_0$ is pulled into the field gradient to be trapped at the point with cylindrical coordinates (z^*, ρ^*).

II. PHYSICAL MODEL

The CM Eq. (5) is derived by assuming that the dividing surface between the dielectric medium and the protein molecule is polarized by the field of external charges $\mathbf{E}_0$ resulting in the macroscopic Maxwell field **E** inside the dielectric medium. The induced dipole is directed opposite to the applied field [Fig. 3(a), negative DEP] when the medium is more polarizable than the particle ($\varepsilon_s > \varepsilon_p$). The dipole moment assigned to an effective sphere

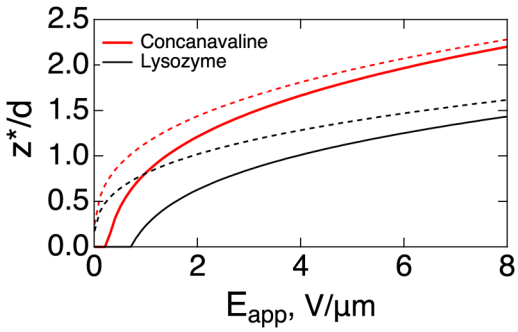

FIG. 2. Energy balancing distance z^* at $\rho = 0$ as a function of the applied field E_{app} for lysozyme and concanavaline proteins (Table I). The dipole approximation [dashed lines, Eq. (8)] converges on the general solution (solid lines) for sufficiently large applied field strengths.

Downloaded from http://pubs.aip.org/aip/jap/article-pdf/doi/10.1063/5.0144564/17001652/164701_1_5.0144564.pdf

Published under an exclusive license by AIP Publishing

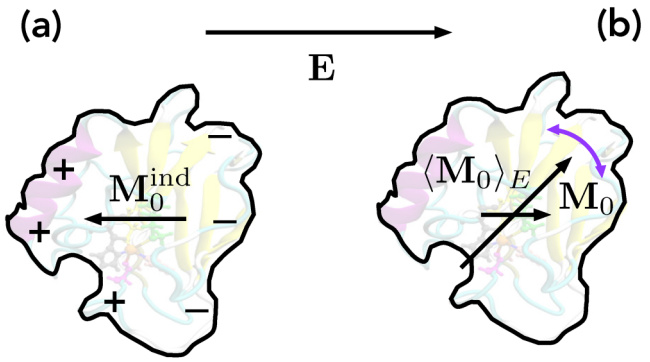

FIG. 3. Schematics of the dipole moment $\mathbf{M}_0^{\mathrm{ind}}$ induced at a polarizable particle (a) and the dipole moment $\langle \mathbf{M}_0 \rangle_E$ averaged over orientations of the permanent dipole moment $\mathbf{M}_0$ in the presence of the external field $\mathbf{E}$ inside the dielectric (b). "+" and "−" in (a) indicate surface charges induced at the dielectric interface. Tumbling of the permanent dipole with the relaxation time τ_p of dielectric β-relaxation results in $\langle \mathbf{M}_0 \rangle = 0$ in the absence of an external electric field. The average dipole $\langle \mathbf{M}_0 \rangle_E$ in the presence of the field is oriented along the field, while the induced dipole $\mathbf{M}_0^{\mathrm{ind}}$ is opposite to the field when the solvent is more polarizable than the protein.

representing the solute becomes[8,9]

$$\mathbf{M}_0^{\mathrm{ind}} = -3\varepsilon_0\Omega_0 \frac{\varepsilon_s - \varepsilon_p}{2\varepsilon_s + \varepsilon_p}\mathbf{E}. \tag{11}$$

When substituted to Eq. (1), this equation leads to the DEP susceptibility in Eqs. (5) and (6).

An alternative mechanism of inducing a dipole at the particle is through aligning the permanent dipole $\mathbf{M}_0$ along the external field $\mathbf{E}$. Random rotations of $\mathbf{M}_0$ produce $\langle \mathbf{M}_0 \rangle = 0$ in the absence of the field ($E = 0$), but there will be a net average dipole moment $\langle \mathbf{M}_0 \rangle_E$ in the presence of the field [Fig. 3(b)]. This dipole moment is found by applying the first-order perturbation theory in terms of the perturbation $-\mathbf{M} \cdot \mathbf{E}_0$ aligning the solute and liquid dipoles along the field of external charges $\mathbf{E}_0$.[9] The external field acts on the entire dipole of the system

$$\mathbf{M} = \sum_{i=1}^{N_0} \mathbf{M}_{0,i} + \mathbf{M}_s \tag{12}$$

including the dipole moment of the medium (solvent) $\mathbf{M}_s$ and N_0 non-interacting protein dipoles $\mathbf{M}_{0,i}$ (infinite dilution). By neglecting interactions between protein dipoles in solution, one can apply the first-order perturbation theory[21,38] to find the magnitude of the individual protein dipole aligned along the field

$$\langle \mathbf{M}_0 \rangle_E = \frac{\varepsilon_s}{3}\beta \langle \mathbf{M}_0 \cdot \mathbf{M} \rangle \mathbf{E} = \frac{\varepsilon_s}{3}\beta\chi_c M_0^2 \mathbf{E}. \tag{13}$$

Here, the statistical average $\langle \cdots \rangle$ refers to no applied electric field and the macroscopic connection $\mathbf{E}_0 = \varepsilon_s \mathbf{E}$ between $\mathbf{E}_0$ and $\mathbf{E}$ through the medium dielectric constant ε_s has been adopted. Equation (13) assumes that the induced dipole is a small fraction of the permanent dipole of the protein (linear response). This assumption can be violated in very strong fields: one gets $\langle M_0 \rangle_E / M_0 \simeq 0.2$ at $E \simeq 0.1$ V/μm and $M_0 = 100$ D. The replacement of the left-hand-side of Eq. (13) with the Langevin function[39] is required in strong fields.

The average dipole in Eq. (13) aligned along the field is specified by statistical correlations between the particle dipole $\mathbf{M}_0$ and the total dipole moment of the sample $\mathbf{M}$ [first relation in Eq. (13)]. The cross correlations, $\langle \mathbf{M}_0 \cdot \mathbf{M}_s \rangle$, between $\mathbf{M}_0$ and the solvent component of the sample dipole $\mathbf{M}_s$ are accounted for by the cavity-field susceptibility[21] χ_c in the second relation in Eq. (13). This susceptibility is defined as the ratio of the electric field inside the solute (cavity) E_c and the field of external charges E_0 (vacuum field). The cavity-field susceptibility is difficult to measure directly, but it was found to be close to unity, $\chi_c \simeq 1.0 - 1.4$, in numerical simulations of proteins[31,32] and can be dropped in practical calculations.

The vacuum field E_0 of external charges sets up the perturbation used in statistical–mechanical formulations of the theory. It needs to be related to the Maxwell field inside the dielectric E for practical calculations. The simple connection $\varepsilon_s E = E_0$ used here starting from Eq. (1) applies only to equipotential surfaces produced by immersing conductors into dielectrics[40] and becomes inapplicable when interfaces between dielectrics with different dielectric constants are involved in producing E (such as in insulator-based, iDEP, applications). Our present calculations apply only to that former configuration realized in electrode-based (eDEP) devices.[4] One has to realize that DEP requires a gradient of the field E_0 produced by free charges, which are external charges at the metal electrodes and ions in the solution and at interfaces. From this perspective, the connection $\varepsilon_s E = E_0$ does not apply to electrolyte solutions where the dielectric constant enters also the Debye–Hückel screening parameter. The theory should be formulated in terms of E_0 in such applications.

By applying Eq. (13) to Eqs. (1) and (3), one obtains for the dipolar mechanism of DEP (superscript "d"),

$$\chi_{\mathrm{DEP}}^d = \frac{\varepsilon_s^2}{6\varepsilon_0}\beta\chi_c M_0^2 \simeq 50.6\ \varepsilon_s^2 \chi_c M_0^2. \tag{14}$$

The last equation gives the DEP susceptibility in Å^3 assuming $T = 300$ K and M_0 in debye units. The dimensionless polarization factor K in Eq. (4) is given by the dipolar form[31]

$$K_d = \varepsilon_s \chi_c y_0, \tag{15}$$

where

$$y_0 = \beta M_0^2/(9\varepsilon_0\Omega_0) \tag{16}$$

is the dimensionless polarity parameter of the solute. This parameter is far greater than unity for a typical globular protein[32] (Table I). With $\varepsilon_s \simeq 78$ for aqueous solutions of proteins, $K_d \sim 10^3$–10^4 far exceeds $|K_{\mathrm{CM}}| \simeq 0.5$.[21,32] A recent report[28] lists $K = 402$ and 5 for lysozyme and BSA, respectively. The reported trapping fields $E_{\mathrm{trap}} = 2.6$ (Lys) and 5.26 V/μm (BSA)[28] used in

Downloaded from http://pubs.aip.org/aip/jap/article-pdf/doi/10.1063/5.0144564/17001652/164701_1_5.0144564.pdf

Published under an exclusive license by AIP Publishing

Eq. (7) produce $K = 32$ (Lys) and 1.4 (BSA) (Table I footnote). Given that electrolyte screening was not accounted for in experimental estimates, Eq. (7) yielding 0.3 V/μm (Lys) and 0.1 V/μm (BSA) with parameters from Table I provides the low boundary for the capturing field. Based on the current theory and these experimental results, positive DEP has to be expected for proteins and other nanoparticles carrying permanent dipole moments.

An important distinction between the dielectric interface polarization [CM, Fig. 3(a)] and dipolar [Fig. 3(b)] mechanisms of DEP is in the scaling of the force with the particle size. One gets linear scaling with the particle volume, $\propto R_0^3$ [Eq. (6)], in the former case and proportionality to the dipole moment squared, $\propto M_0^2$, in the latter case [Eq. (14)]. Assuming that the dipole moments grow linearly with the particle size,[41] one gets $\chi_{\rm DEP} \propto R_0^2$ when the permanent dipole dominates in the DEP susceptibility. Note that this scaling only specifies a trend since the dipole moment is also affected by the protein symmetry (see IgG in Table I as an example). Nevertheless, different scaling laws should be anticipated and a negative DEP, based on the CM factor, should dominate for large particles of submicron and micron size, while positive DEP is important for asymmetric molecular solutes carrying large permanent dipoles. The condition

$$2\varepsilon_s\chi_c y_0 \simeq 1 \tag{17}$$

reached at increasing the solute size provides the crossover from the positive dipolar DEP to the standard CM mechanism ($K \simeq 0$ when this condition is satisfied). Note that the dipolar alignment and interfacial polarization can mostly be viewed as independent and the overall polarization parameter is a sum of the two contributions allowing a continuous transition between two scaling trends

$$K = K_d + K_{\rm CM}. \tag{18}$$

Since $|K_{\rm CM}| \ll K_d$ for individual proteins, only the dipolar mechanism is considered here. Nevertheless, protein aggregation, increasing the volume of each particle, can lead to the return to the standard CM mechanism of DEP.

There is another essential distinction between $\chi^{\rm CM}_{\rm DEP}$ in Eq. (6) and $\chi^{d}_{\rm DEP}$ in Eq. (14). The former is only weakly temperature dependent, through density and $\varepsilon_s(T)$, whereas the latter is explicitly proportional to the inverse temperature, $\chi^{d}_{\rm DEP} \propto T^{-1}$. This temperature scaling is distinct from both the mechanical force, which is temperature-independent, and the entropic force[7] scaling as $\propto T$. The entropy, $\mathscr{S}_E$, and enthalpy, $\mathscr{H}_E$, of the protein polarization become [see Eq. (1)]

$$T\mathscr{S}_E = \mathscr{F}_E, \quad \mathscr{H}_E = 2\mathscr{F}_E. \tag{19}$$

The temperature scaling characteristic of dipolar DEP will propagate to all parameters derived from the corresponding dielectrophoretic force. For instance, the capture distance in Eq. (9) is also affected by temperature

$$z^* \propto T^{-1/3}. \tag{20}$$

To summarize this section, several key distinctions between $K_{\rm CM}$ and K_d carry full analogy with the well-recognized distinctions between theories of nonpolar (but polarizable) and polar (carrying molecular dipoles) bulk liquids. The former concerns itself with the field induced in a macroscopic polarizable (virtual) cavity carved from a fluid of electronically induced dipoles oriented along the external field. The result is the CM factor appearing in the expression for the dielectric constant of nonpolar liquids.[2,39] In contrast, the theory of polar liquids operates with permanent liquid dipoles $\mathbf{m}$ experiencing constant rotations due to thermal agitation and averaging to zero in the absence of an external field, $\langle \mathbf{m} \rangle = 0$. The permanent dipole of the polar liquid induced by an external field and not averaged to zero is found by perturbation theory formulated similarly to Eq. (13). Such a perturbation description yields the liquid dielectric constant through the Onsager and Kirkwood–Onsager equations[38,39] operating in terms of the dimensionless density of liquid dipoles $y = \beta\rho m^2/(9\varepsilon_0)$, where ρ is the liquid number density. The parameter y_0 appearing in Eqs. (15) and (16) is an obvious analog of this standard formulation applied to a single protein dipole occupying the volume Ω_0.

III. NANOTRAP MODEL

Nanometer to micrometer holes drilled in substrates or membranes have been used for the manipulation of biomolecules.[34,42–45] The geometry shown in Fig. 1 assumes that the hole diameter is much larger than the membrane thickness, leading to a limit of a circular aperture in an infinitely thin conducting plate. However, the solution for the electrostatic potential in oblate spheroidal coordinates[40] used here applies to an arbitrary hourglass-shaped nanopore[35] when the restriction of an infinitely thin membrane used here is lifted. A solution for the geometry of a thin one-dimensional nanogap[16] can be obtained along similar lines. Nanohole arrays have been employed elsewhere for protein[46] and DNA[47] DEP. In those applications, capture is achieved at the hole opening and the geometry of the hole and the inter-electrode space become significant. A simplified geometry used here aims at providing an analytical framework allowing asymptotic solutions.

The field $E_{\rm app}$ between two capacitor plates leaks through the opening in the top conduction plate creating the field gradient in the space above it (Fig. 1). By using the oblate spheroidal coordinates as defined in Ref. 48, the cylindrical coordinates z, ρ are transformed to ξ_1, ξ_2,

$$\rho = \sqrt{(\xi_1^2 + d^2)(1 - \xi_2^2)}, \quad z = \xi_1\xi_2. \tag{21}$$

The solution of the Poisson equation for the electrostatic potential $\phi(\xi_1, \xi_2)$ in the upper half-plane is given in coordinates ξ_1, ξ_2 as follows (see the supplementary material for details):

$$\phi(\xi_1, \xi_2) = \frac{E_{\rm app}}{\pi}\xi_2\xi_1\left[\frac{d}{\xi_1} - \operatorname{atan}\frac{d}{\xi_1}\right]. \tag{22}$$

Downloaded from http://pubs.aip.org/aip/jap/article-pdf/doi/10.1063/5.0144564/17001652/164701_1_5.0144564.pdf

Published under an exclusive license by AIP Publishing

The z- and ρ-components of the electric field follow by taking the potential gradient (see the supplementary material),

$$\frac{\pi E_z}{E_{\rm app}} = \operatorname{atan}\frac{d}{\xi_1} - \frac{d\xi_1}{\xi_1^2 + d^2\xi_2^2},$$
$$\frac{\pi E_\rho}{E_{\rm app}} = -\frac{\rho z}{\xi_1^2 + d^2\xi_2^2}\left[\frac{d}{\xi_1} - \frac{\xi_1 d}{\xi_1^2 + d^2} + \left(1 - \frac{d}{\xi_1}\right)\operatorname{atan}\frac{d}{\xi_1}\right]. \quad (23)$$

At large distances from the hole, the electrostatic field becomes the field of a dipole. The field along the z axis becomes

$$E = E_z = \frac{2d^2}{3\pi z^3}E_{\rm app}. \quad (24)$$

This expression is used to derive the trapping distance z^* in Eq. (8) as shown in Fig. 2.

From two field projections in Eq. (23), one can arrive at the magnitude of the field squared,

$$\frac{\pi^2 E^2}{E_{\rm app}^2} = \operatorname{atan}^2\frac{d}{\xi_1} + \frac{d^2}{\xi_1^2 + d^2\xi_2^2}\left(1 - \frac{d^2\xi_2^2}{\xi_1^2 + d^2} - \frac{2\xi_1}{d}\operatorname{atan}\frac{d}{\xi_1}\right). \quad (25)$$

This scalar function is used to calculate the gradient of E^2 to arrive at the DEP force in Eq. (3).

When the protein is driven by the hydrodynamic flow with the velocity v along the x-axis parallel to the plate, the trapping position in the capacitor x, y- plane can be determined by equating the x-projection of the DEP force (Fig. 1) with the hydrodynamic drag[10,49] experienced by the protein in the uniform flow along the x axis,

$$\frac{\varepsilon_0\varepsilon_s}{3\eta}R_0^2 K\nabla_x E^2 = -v, \quad (26)$$

where η is the liquid's shear viscosity. The trapping contour determined by this condition with E^2 from Eq. (25) is shown in Fig. 4. An oval shape of the trapping contour is a reflection of the dipolar symmetry of the electric field produced by the spherical aperture.

IV. PROTEIN DEP

The DEP susceptibility $\chi_{\rm DEP}$ has never been directly measured (see, however, Ref. 28) and alternative sources of experimental input need to be sought. The access to K_d and $\chi^d_{\rm DEP}$ is allowed by the observation[31,32] that the factor $\chi_c y_0$ that defines K_d in Eq. (15) also enters the expression for the dielectric constant of a dilute solution of N_0 dipolar particles carrying permanent dipole moments M_0 and dissolved in the polar solvent with the bulk dielectric constant ε_s. Dielectric experiments are typically performed with external fields oscillating with the circular frequency ω and applied to a plane capacitor. Rotations of the solute dipole in solution are reflected by the dielectric relaxation process known as β-dispersion.[50–52]

The dielectric function of the medium $\varepsilon(\omega)$ becomes the static dielectric constant ε_s in the limit $\omega \to 0$: $\varepsilon_s = \mathrm{Re}[\varepsilon(\omega \to 0)]$. The high-frequency limit of the dielectric function is $\varepsilon_\infty = \mathrm{Re}[\varepsilon(\omega \to \infty)]$ defining the dielectric increment $\Delta\varepsilon(\omega) = \varepsilon(\omega) - \varepsilon_\infty$. The

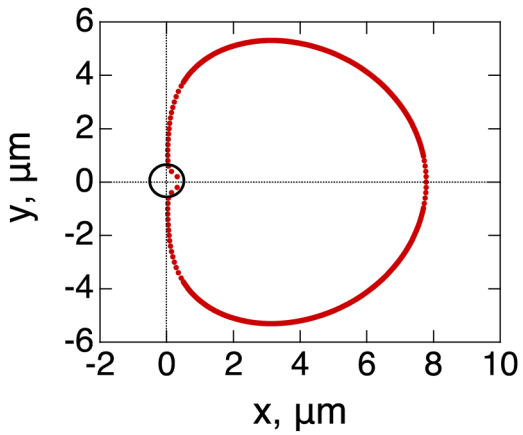

FIG. 4. Trapping contour in the $x - y$ plane for $E_{\rm app} = 1$ V/μm and $z = 1$ μm. The calculations are carried out for lysozyme (Table I) with $v = 10$ cm/s and $\eta = 1$ cP for water at normal conditions used in Eq. (26). The black circle indicates the aperture with $d = 1$ μm.

increment of the dielectric function of solution over that of the pure solvent, $\Delta\varepsilon_{\rm sol}(\omega) = \varepsilon_{\rm sol}(\omega) - \varepsilon(\omega)$, is given[32] in terms of the volume fraction of solutes $\eta_0 = N_0\Omega_0/\Omega$ (Ω is the solution volume),

$$\frac{\Delta\varepsilon_{\rm sol}(\omega)}{\eta_0} + \Delta\varepsilon(\omega) = \frac{9}{2}y_0(\omega)(2\chi_c(\omega) - 1). \quad (27)$$

Here, the solute polarity parameter y_0 [Eq. (16)] and the cavity-field susceptibility χ_c [Eq. (13)] both become functions of ω. Given that in many practical situations $(2\chi_c(\omega) - 1 \simeq 1$, the equation for the dielectric increment of solution simplifies[32] at small particle concentrations, $\eta_0 \to 0$, when the second term on the left-hand side can be dropped. One obtains in this limit

$$\frac{\Delta\varepsilon_{\rm sol}}{c_0} = 9.14 \times 10^{-5} M_0^2. \quad (28)$$

The numerical factor in this equation is calculated for c_0 in mM and the protein dipole in debye units. This is an alternative form of Oncley's equation[53] connecting the dielectric increment to protein's dipole. The dipolar DEP factor is obtained by substituting Eq. (28) to Eq. (15) with the result ($\chi_c \simeq 1$),

$$K_d = \frac{2}{9}\varepsilon_s(\Delta\varepsilon_{\rm sol}/\eta_0 + \Delta\varepsilon). \quad (29)$$

The limit of Eq. (28) implies dropping the second summand in the brackets in this equation. One obtains in this limit

$$K_d \simeq 36.9\frac{\varepsilon_s}{\Omega_0}\frac{\Delta\varepsilon_{\rm sol}}{c_0}, \quad (30)$$

where Ω_0 is in nm^3 and c_0 is in mM.

Downloaded from http://pubs.aip.org/aip/jap/article-pdf/doi/10.1063/5.0144564/17001652/164701_1_5.0144564.pdf

Published under an exclusive license by AIP Publishing

When the frequency dependence is maintained in Eq. (29), it predicts a crossover in the sign of $K_d(\omega)$[15,16] when $\Delta\varepsilon_{sol}(\omega)$ becomes negative at frequencies comparable with the frequency of tumbling of the protein dipole ($\nu = \omega/(2\pi) \sim 10$ MHz). This relaxation process is classified as β-dielectric relaxation of protein solutions characterized by the dielectric increment $\Delta\varepsilon_\beta$. There is a higher-frequency, ~100 MHz,[50,52,54,55] relaxation process called δ-relaxation. Its origin has been attributed to cross correlations between the protein and water dipoles.[56–59] From this assignment, the cavity-field susceptibility can be estimated from the ratio of the dielectric increment for δ- and β-relaxation processes,[32]

$$\chi_c = 1 + \frac{\Delta\varepsilon_\delta}{2\Delta\varepsilon_\beta}. \tag{31}$$

The data for $\Delta\varepsilon_\delta$ and $\Delta\varepsilon_\beta$[54,60] are used to estimate χ_c in Table I (see the supplementary material for details). The resulting χ_c is close to unity and can be dropped from calculations of K_d. This simple result is not trivial since the cavity susceptibility of the protein–water interface turns out to be significantly higher than the prescription of dielectric theories,[38,39]

$$\chi_c = 3/(2\varepsilon_s + \varepsilon_p). \tag{32}$$

The parameters required to calculate the dipolar polarization factor K_d [Eq. (29)] are taken from solution dielectric data for ubiquitin,[58] lysozyme,[61] and IgG[60] (as is common in dielectric literature,[62] fitting of dielectric spectra is involved in extracting the static dielectric data). The dielectric data for the rest of proteins in Table I are from Refs. 11 and 12. The protein radii were taken from Ref. 32 and additionally calculated by using the software McVol[63] (see the supplementary material). The dipole moments are from Refs. 64–66 and water's dielectric parameters are from Ref. 67.

V. DISCUSSION

The discussion presented here distinguishes between two mechanisms of nanometer-scale DEP: polarization of bound charges at the dielectric interface (CM factor) and alignment of the solute's molecular permanent dipole along the external field (dipolar DEP). These two mechanisms lead to numerically different dimensionless polarization parameters K entering the DEP susceptibility [Eq. (4)]: $|K_{CM}| \simeq 0.5$ and the dipolar parameter K_d of the order 10^3–10^4 for proteins studied here (Table I). A substantially larger value of K_d allows protein trapping on nanopore devices. As discussed above, the scaling of K with the particle size is different for two mechanisms: $\propto R_0^3$ for dielectric polarization and $\propto R_0^2$ for the dipolar mechanism. The latter result is qualitatively confirmed by the data accumulated in Table I. Figure 5 shows $\Omega_0 K_d$ vs R_0 for proteins listed in Table I. The scaling exponent in the scaling law $\chi_{DEP} \propto R_0^\alpha$ is $\alpha \simeq 2.03$. The linear regression shown in Fig. 5 allows one to estimate χ_{DEP} in Eq. (4) from the protein radius.

Two physically significant factors allow large values of the polarization parameter K for proteins: (i) a large dipole moment of a typical globular protein and (ii) a large value of the cavity-field susceptibility $\chi_c \simeq 1$ far exceeding the dielectric estimate in Eq. (32). A large cavity-field susceptibility is characteristic of the protein–water interface, which is much distinct from what is anticipated in theories of dielectric interfaces. The main physical reason for unusual dielectric properties is a large density of positive a negative ionized residues at the protein surface.[41] These residues orient the surface water into clusters (nanodomains[68]) with dipole moments directed along the local electric field. This physical situation is illustrated in Fig. 6 where two domains, next to a positive and a negative surface charge, are shown. The cavity susceptibility results from the cross correlation of the protein, $\mathbf{M}_0$, and solvent,

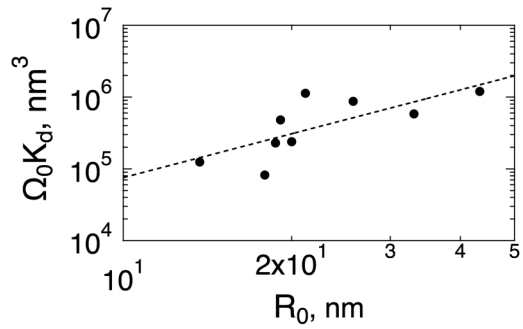

FIG. 5. $\Omega_0 K_d$ vs R_0 (logarithmic scale) for proteins listed in Table I. The dashed line is the linear fit showing the scaling exponent equal to 2.03. The dashed line shows the linear regression: $\ln \Omega_0 K_d = 6.56 + 2.03 \ln R_0$.

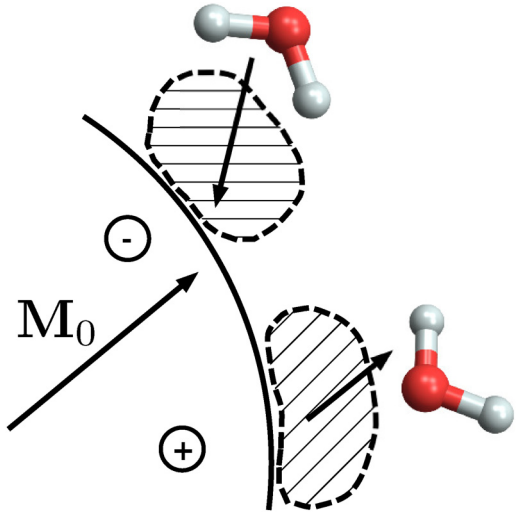

FIG. 6. Schematic drawing of dipolar water domains at the protein surface. Surface cations and anions rotate the domain dipoles outward and inward from the dividing surface, respectively. The water molecules shown in the plot indicate their preferential orientations within the domains. Releasing O–H bonds toward a surface anion requires less frustration of interfacial waters than pointing O–H bonds toward the bulk. Cross correlations of the protein dipole $\mathbf{M}_0$ and the surface water dipoles determine the deviation of χ_c from unity [Eq. (33)].

Downloaded from http://pubs.aip.org/aip/jap/article-pdf/doi/10.1063/5.0144564/17001652/164701_1_5.0144564.pdf

Published under an exclusive license by AIP Publishing

$\mathbf{M}_s$, dipole moments[21] [Eqs. (12) and (13)],

$$\chi_c = 1 + \langle \delta\mathbf{M}_0 \cdot \delta\mathbf{M}_s \rangle / \langle \delta\mathbf{M}_0 \cdot \delta\mathbf{M}_0 \rangle, \tag{33}$$

where for a protein permanent dipole spanning isotropic orientations, one gets $\langle \delta\mathbf{M}_0 \cdot \delta\mathbf{M}_0 \rangle = M_0^2$.

The deviation of the cavity-field susceptibility from $\chi_c = 1$ is, therefore, caused by cross correlations between the protein dipole and water dipoles in protein's hydration shell. Such correlations are substantial when orientations of interfacial dipoles are predominantly caused by the dipolar field of the solute as assumed in the standard dielectric theories.[39] The resulting negative cross correlations lead to $\chi_c \ll 1$ [Eq. (32)]. When, on the contrary, the dipolar orientations and their fluctuations are governed by the local fields of the surface charged residues, the domains with opposite local orientations tend to cancel each other resulting in $\chi_c \simeq 1$ (Fig. 6). The dipoles within domains next to cations and anions can be different given that releasing O–H bonds next to a surface anion requires lower stress and frustration than turning O–H bonds toward the bulk near a surface cation (Fig. 6). The compensation between the domains is incomplete and χ_c can even slightly exceed unity as is empirically found (Table I). These estimates are based on the assumption that δ-relaxation of the protein solution reflects cross correlations between the protein and hydration water dipoles [Eqs. (31) and (33)], which still requires experimental scrutiny. Nevertheless, the appearance of the cavity-field susceptibility consistent with estimates listed in Table I also follows from the concentration dependence[69] of THz radiation absorption by protein solutions.[70]

There are a number of observable qualitative distinctions between induction and dipolar mechanisms of DEP. As mentioned, the dipolar DEP predicts a significant dependence on temperature, $K_d \propto T^{-1}$, with the corresponding temperature dependence affecting the trapping distance [Eq. (20)]. Given that $K_d \propto M_0^2$ [Eqs. (15) and (16)], any physical property altering the protein dipole, such as mutations or unfolding, should be reflected by the DEP susceptibility. In particular, the protein dipole moment is affected by pH of the solution[71] and corresponding effects of pH on protein DEP have been reported in the past.[23,72,73] Our calculations indicate that changing pH should substantially affect the DEP susceptibility. Figure 7 shows the dependence of the DEP polarization parameter K_d on the solution pH calculated from the data available for the BSA protein.[71,74]

The results presented here discuss trapping of proteins by static inhomogeneous electric fields. This discussion is extended to oscillatory fields by allowing the frequency-dependent dielectric function for the solvent $\varepsilon_s(\omega)$ and the corresponding frequency-dependent protein dipole moment density $y_0(\omega)$ in Eq. (16).[31,32] The frequency dependence of $y_0(\omega)$ is caused by tumbling of the protein dipole with the relaxation time τ_p of β-relaxation in dielectric spectroscopy. For simplest exponential relaxation of the protein dipole, one arrives at the Debye relaxation form

$$y_0(\omega) = y_0\left(1 - i\omega\tau_p\right)^{-1}. \tag{34}$$

Alternatively, $y_0(\omega)$ follows from Eq. (27), which can involve more complex relaxation functions for the protein dipole. The change in the sign of the right-hand side of Eq. (27) at high frequencies will produce the crossover from positive to negative DEP. The change of sign of DEP is a direct consequence of dynamic freezing of protein rotations at high frequencies.

The question of the minimum field gradient $|\nabla E^2|$ required for protein trapping has been raised in a number of recent reviews.[23,26,29] The values typically estimated[26] for the CM polarization mechanism are of the order of 10^{21} V/m^3. Capture of proteins often requires much lower field gradients,[26,28] sometimes down to 10^{12} V/m^3. Figure 8 presents field gradients for the nanopore trapping geometry at the uniform field in the lower part of the capacitor equal to $E_{app} = 1$ V/μm. The field gradients shown in Fig. 8 are calculated for proteins from Table I at the capturing distance z^* determined from the energy match condition specified by Eq. (7). The field gradient of the order of 10^{17} V/m^3 is required for the dipolar mechanism of DEP at the adopted strength of the capacitor field $E_{app} = 1$ V/μm responsible for the field gradient at the pore opening: $|\nabla E^2|$ scales linearly with E_{app}^2 [Eq. (25)]. Experimentally, the field gradient of $|\nabla E^2| \simeq 10^{17}$ V^2/m^3 was reported for BSA capturing.[75]

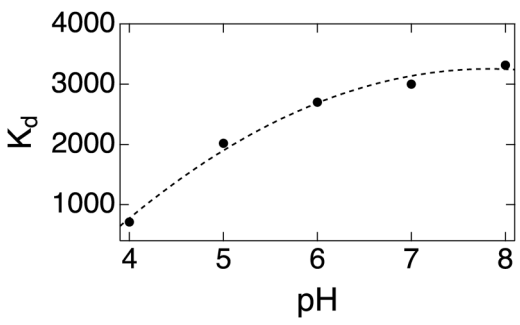

FIG. 7. K_d vs pH for BSA protein.

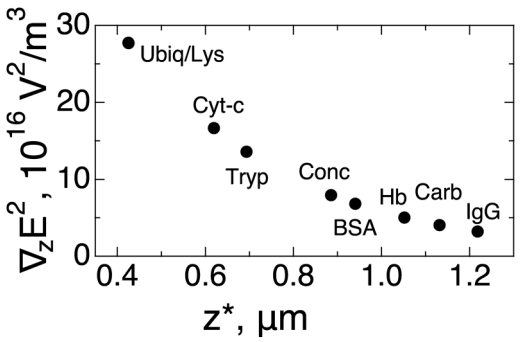

FIG. 8. $\nabla_z E^2$ vs z^* for the proteins listed in Table I. The calculations are done at $E_{app} = 1$ V/μm and $d = 1$ μm.

Downloaded from http://pubs.aip.org/aip/jap/article-pdf/doi/10.1063/5.0144564/17001652/164701_1_5.0144564.pdf

Published under an exclusive license by AIP Publishing

VI. CONCLUSIONS

DEP is a potentially powerful method to trap proteins and we have demonstrated that protein trapping can be achieved on a nanopore of micrometer length scale with the electric field strength and gradient values accessible to experimental conditions. The dipolar mechanism of DEP can be viewed as dominant for proteins given the present state of theory and empirical data.

SUPPLEMENTARY MATERIAL

See the supplementary material for derivation of equations presented in the text, maps of electrostatic potential around the nanotrap, and parameters for proteins used in the calculations.

ACKNOWLEDGMENTS

This research was supported by the National Science Foundation (NSF) (No. CHE-2154465). We are grateful to Dr. S. Zavatski for providing us with additional data from Ref. 28.

AUTHOR DECLARATIONS

Conflict of Interest

The authors have no conflicts to disclose.

Author Contributions

Taylor Colburn: Formal analysis (equal); Software (lead); Visualization (lead); Writing – review & editing (equal). **Dmitry V. Matyushov:** Conceptualization (lead); Formal analysis (equal); Project administration (lead); Writing – review & editing (equal).

DATA AVAILABILITY

The data that support the findings are available from the authors upon request.

REFERENCES

[1]H. A. Pohl, *Dielectrophoresis. The Behavior of Neutral Matter in Nonuniform Electric Fields* (Cambridge University Press, Cambridge, 1978).
[2]B. K. P. Scaife, *Principles of Dielectrics* (Clarendon Press, Oxford, 1998).
[3]R. Pethig, J. Electrochem. Soc. **164**, B3049 (2017).
[4]R. Pethig, *Dielectrophoresis. Theory, Methodology and Biological Applications* (Wiley, Hoboken, NJ, 2017).
[5]S. R. de Groot and P. Mazur, *Nonequilibrium Thermodynamics* (North-Holland Publishing Co., Amsterdam, 1963).
[6]D. Reguera, J. M. Rubí, and J. M. G. Vilar, J. Phys. Chem. B **109**, 21502 (2005).
[7]J. Israelachvili, *Intermolecular & Surface Forces* (Academic Press, Amsterdam, 1991).
[8]D. V. Matyushov, *Manual for Theoretical Chemistry* (World Scientific Publishing Co. Pte. Ltd., New Jersey, 2021).
[9]J. D. Jackson, *Classical Electrodynamics*, 3rd ed. (Wiley, New York, 1999).
[10]X. Xuan, Electrophoresis **40**, 2484 (2019).
[11]R. Hölzel and R. Pethig, Micromachines **11**, 533 (2020).
[12]R. Hölzel and R. Pethig, Electrophoresis **42**, 513 (2020).
[13]A. Castellanos, A. Ramos, A. González, N. G. Green, and H. Morgan, J. Phys. D: Appl. Phys. **36**, 2584 (2003).
[14]A. Nakano, T.-C. Chao, F. Camacho-Alanis, and A. Ros, Electrophoresis **32**, 2314 (2011).
[15]Z. Cao, Y. Zhu, Y. Liu, S. Dong, X. Chen, F. Bai, S. Song, and J. Fu, Small **14**, 1703265 (2018).
[16]A. Barik, X. Chen, and S.-H. Oh, Nano Lett. **16**, 6317 (2016).
[17]A. Henriksson, P. Neubauer, and M. Birkholz, Biosensors **12**, 784 (2022).
[18]T. Yamamoto and T. Fujii, Nanotechnology **18**, 495503 (2007).
[19]M. Washizu, S. Suzuki, O. Kurosawa, T. Nishizaka, and T. Shinohara, IEEE Trans. Ind. Appl. **30**, 835 (1994).
[20]R. W. Clarke, S. S. White, D. Zhou, L. Ying, and D. Klenerman, Angew. Chem. Int. Ed. **44**, 3747 (2005).
[21]D. V. Matyushov, J. Chem. Phys. **136**, 085102 (2012).
[22]R. Hölzel, N. Calander, Z. Chiragwandi, M. Willander, and F. F. Bier, Phys. Rev. Lett. **95**, 128102 (2005).
[23]A. Nakano and A. Ros, Electrophoresis **34**, 1085 (2013).
[24]E.-M. Laux, X. Knigge, F. F. Bier, C. Wenger, and R. Hölzel, Electrophoresis **36**, 2094 (2015).
[25]D. Kim, M. Sonker, and A. Ros, Anal. Chem. **91**, 277 (2019).
[26]M. A. Hayes, Anal. Bioanal. Chem. **412**, 3801 (2020).
[27]B. H. Lapizco-Encinas, Cur. Opinion Chem. Eng. **29**, 9 (2020).
[28]S. Zavatski, H. Bandarenka, and O. J. F. Martin, Anal. Chem. **95**, 2958 (2023).
[29]R. Pethig, Micromachines **13**, 261 (2022).
[30]D. V. Matyushov, Biomicrofluidics **13**, 064106 (2019).
[31]S. S. Seyedi and D. V. Matyushov, J. Phys. Chem. B **122**, 9119 (2018).
[32]M. Heyden and D. V. Matyushov, J. Phys. Chem. B **124**, 11634 (2020).
[33]A. Ramos, H. Morgan, N. G. Green, and A. Castellanos, J. Phys. D: Appl. Phys. **31**, 2338 (1999).
[34]H. Yang and G. Qing, Chem. Phys. Rev. **2**, 021306 (2021).
[35]S. W. Kowalczyk, A. Y. Grosberg, Y. Rabin, and C. Dekker, Nanotechnology **22**, 315101 (2011).
[36]M. Chinappi, M. Yamaji, R. Kawano, and F. Cecconi, ACS Nano **14**, 15816 (2020).
[37]P. García-Sánchez, J. E. Flores-Mena, and A. Ramos, Micromachines **10**, 100 (2019).
[38]H. Fröhlich, *Theory of Dielectrics* (Oxford University Press, Oxford, 1958).
[39]C. J. F. Böttcher, *Theory of Electric Polarization, Vol. 1: Dielectrics in Static Fields* (Elsevier, Amsterdam, 1973).
[40]L. D. Landau and E. M. Lifshitz, *Electrodynamics of Continuous Media* (Pergamon, Oxford, 1984).
[41]D. J. Barlow and J. M. Thornton, Biopolymers **25**, 1717 (1986).
[42]C. Dekker, Nat. Nanotechnol. **2**, 209 (2007).
[43]M. Muthukumar, *Polymer Translocation* (CRC Press, Boca Raton, FL, 2011).
[44]A. Han, G. Schürmann, G. Mondin, R. A. Bitterli, N. G. Hegelbach, N. F. Rooij, and U. Staufer, Appl. Phys. Lett. **88**, 093901 (2006).
[45]Y. Wu and J. J. Gooding, Chem. Soc. Rev. **51**, 3862 (2022).
[46]A. Barik, L. M. Otto, D. Yoo, J. Jose, T. W. Johnson, and S.-H. Oh, Nano Lett. **14**, 2006 (2014).
[47]K. J. Freedman, L. M. Otto, A. P. Ivanov, A. Barik, S.-H. Oh, and J. B. Edel, Nat. Comm. **7**, 10217 (2016).
[48]P. M. Morse and H. Feshbach, *Methods of Theoretical Physics* (McGraw Hill Book Co., Boston, MA, 1953), Vol. Part I.
[49]H. A. Pohl, J. Appl. Phys. **22**, 869 (1951).
[50]E. H. Grant, R. J. Sheppard, and G. P. South, *Dielectric Behaviour of Biological Molecules in Solution* (Clarendon Press, Oxford, 1978).
[51]S. Takashima, *Electrical Properties of Biopolymers and Membranes* (Adam Hilger, Bristol, 1989).
[52]R. Pethig, Ann. Rev. Phys. Chem. **43**, 177 (1992).
[53]J. L. Oncley, Chem. Rev. **30**, 433 (1942).
[54]N. Miura, N. Asaka, N. Shinyashiki, and S. Mashimo, Biopolymers **34**, 357 (1994).
[55]M. Wolf, R. Gulich, P. Lunkenheimer, and A. Loidl, Biochim. Biophys. Acta **1824**, 723 (2012).
[56]G. Loffler, H. Schreiber, and O. Steinhauser, J. Mol. Biol. **270**, 520 (1997).
[57]S. Boresch, P. Höchtl, and O. Steinhauser, J. Phys. Chem. B **104**, 8743 (2000).

Downloaded from http://pubs.aip.org/aip/jap/article-pdf/doi/10.1063/5.0144564/17001652/164701_1_5.0144564.pdf

Published under an exclusive license by AIP Publishing

[58]A. Knocks and H. Weingärtner, J. Phys. Chem. B **105**, 3635 (2001).
[59]P. Honegger, O. Steinhauser, and C. Schröder, J. Phys. Chem. Lett. **14**, 609 (2023).
[60]Y. Hayashi, N. Miura, J. Isobe, N. Shinyashiki, and S. Yagihara, Biophys. J. **79**, 1023 (2000).
[61]C. Cametti, S. Marchetti, C. M. C. Gambi, and G. Onori, J. Phys. Chem. B **115**, 7144 (2011).
[62]C. J. F. Böttcher, *Theory of Electric Polarization. Dielectrics in Time-Dependent Fields* (Elsevier, 1973), Vol. 2.
[63]M. S. Till and G. M. Ullmann, J. Mol. Mod. **16**, 419 (2010).
[64]S. Takashima and K. Asami, Biopolymers **33**, 59 (1993).
[65]S. Takashima, Biophys. J. **64**, 1550 (1993).
[66]J. Antosiewicz, Biophys. J. **69**, 1344 (1995).
[67]N. Q. Vinh, M. S. Sherwin, S. J. Allen, D. K. George, A. J. Rahmani, and K. W. Plaxco, J. Chem. Phys. **142**, 164502 (2015).
[68]D. R. Martin and D. V. Matyushov, J. Phys. Chem. Lett. **6**, 407 (2015).
[69]F. Novelli, S. Ostovar Pour, J. Tollerud, A. Roozbeh, D. R. T. Appadoo, E. W. Blanch, and J. A. Davis, J. Phys. Chem. B **121**, 4810 (2017).
[70]D. R. Martin and D. V. Matyushov, J. Chem. Phys. **146**, 084502 (2017).
[71]S. Takashima, J. Phys. Chem. **69**, 2281 (1965).
[72]A. Gencoglu, F. Camacho-Alanis, V. T. Nguyen, A. Nakano, A. Ros, and A. R. Minerick, Electrophoresis **32**, 2436 (2011).
[73]A. Nakano, F. Camacho-Alanis, T.-C. Chao, and A. Ros, Biomicrofluidics **6**, 034108 (2012).
[74]S. Yadav, S. J. Shire, and D. S. Kalonia, Pharm. Res. **28**, 1973 (2011).
[75]F. Camacho-Alanis, L. Gan, and A. Ros, Sens. Actuators B **173**, 668 (2012).

Downloaded from http://pubs.aip.org/aip/jap/article-pdf/doi/10.1063/5.0144564/17001652/164701_1_5.0144564.pdf

Published under an exclusive license by AIP Publishing